

The influence of noble-metal-containing cathodes on the electrochemical performance of anode-supported SOFCs

V.A.C. Haanappel*, D. Rutenbeck, A. Mai, S. Uhlenbruck, D. Sebold, H. Wesemeyer,
B. Röwekamp, C. Tropartz, F. Tietz

Institute for Materials and Processes in Energy Systems, Forschungszentrum Jülich, 52425 Jülich, Germany

Received 1 July 2003; accepted 27 November 2003

Abstract

In order to enhance the catalytic activity of the cathode for oxygen reduction and thus to increase the electrochemical performance of planar anode-supported solid oxide fuel cells, Pd, Ag, or Pt was added to the cathode. Four routes were used to add these noble metals: infiltration of the cathode with a Pd solution, deposition of Pt on the electrolyte surface, mixing of $\text{La}_{0.65}\text{Sr}_{0.30}\text{MnO}_3$ (LSM) and YSZ cathode powders with different metal precursors (Pt and Pd black, Pd on activated carbon, Ag powder, Ag_2O , Ag acetate, Ag citrate, Ag_2CO_3 , colloidal Ag, AgNO_3), and synthesis of LSM powder with the addition of AgNO_3 .

Between 750 and 900 °C no electrocatalytic effect occurred with respect to the presence of Pt, either added by deposition on the electrolyte or by mixing with cathode powders. Infiltration of the cathode with a Pd solution or mixing with Pd black did not result in a positive effect either. A catalytic effect was only found with Pd on activated carbon and in particular at lower temperatures.

Cells prepared with Ag powder and Ag_2O showed an improved electrochemical performance compared to Ag-free cells sintered at the same temperature (920 °C). However, in comparison to Ag-free cells sintered at the standard temperature (1100 °C) lower current densities were measured. This can be explained by a weak contact between electrolyte and cathode functional layer and an insufficiently sintered cathode. A detrimental effect was observed regarding the addition of the other Ag precursors. Thermal decomposition of these precursors resulted in the formation of large pores in the cathode.

© 2003 Elsevier B.V. All rights reserved.

Keywords: Solid oxide fuel cells (SOFCs); Noble metals; Cathode; LSM; Microstructure

1. Introduction

Solid oxide fuel cell (SOFC) systems cannot yet compete with conventional combustion systems regarding their investment costs and durability. Research is still needed in order to achieve an attractive return on investment of the SOFC systems. This means that efforts have to be concentrated on reducing production costs and improving performance and durability.

With respect to these problems, one of the main targets is to lower the operating temperature, resulting in reduced sealing and corrosion problems and an improved long-term stability. In addition, cheaper materials for interconnects and manifolds could be used, resulting in lower investment costs. However, to maintain the desired power density at lower operating temperatures, an improvement of the electrochemi-

cal performance is needed. Significant progress in this direction was already made several years ago by the introduction of anode-supported instead of electrolyte-supported cells [1]. Today, the cathode is the limiting component for a further step forward. One way to overcome this limitation may be to improve the oxygen reduction step by adding noble metals, e.g. Pd, Ag, or Pt, to the cathode. An overview of different studies regarding the influence of small amounts of noble metals on the electrochemical characterization of SOFC cathodes is given in Table 1.

Concerning the catalytic effects of small amounts of palladium on the electrochemical performance of single cells, only a small number of studies can be found in the literature [2–4]. It was concluded that the addition of palladium to the cathode results in an improvement of the performance. Erning et al. [2] reported that small additions of palladium lower the activation energy of the oxygen reduction reaction, whereas the current density at various overpotentials was increased by almost one order of magnitude. These conclusions were based on the Tafel plots

* Corresponding author. Tel.: +49-2461-614656;

fax: +49-2461-616770.

E-mail address: v.haanappel@fz-juelich.de (V.A.C. Haanappel).

Table 1

Overview of different studies regarding the influence of small amounts of noble metals on the electrochemical characteristics of SOFC cathodes

Measurement	Cathode composition	Method of addition	Loading	Temperature (°C)	Effect	Reference
C–V + ac impedance	La _{0.84} Sr _{0.16} MnO ₃ (50 μm) on 8YSZ (130 μm) (active area: 0.8 cm ²)	Metallic Pd _{aqueous} on electrolyte (8YSZ); Pd chloride _{solution} on electrolyte (8YSZ)	≤100 μg/cm ²	800	+	[2]
ac impedance	La _{0.6} Sr _{0.4} Fe _{0.8} Co _{0.2} O ₃ (n.g. μm) on Ce _{0.9} Gd _{0.1} O _{1.95} (5 μm) (both sides) (active area: n.g. cm ²)	Pd nitrate _{solution} impregnation of LSF cathode	0–15 μg/cm ²	400–750	+	[3]
C–V	La _{0.6} Sr _{0.4} Fe _{0.8} Co _{0.2} O ₃ (≥10 μm) on Ce _{0.9} Gd _{0.1} O _{1.95} (5 μm) (anode-supported) (active area: 2.5 cm ²)	Pd nitrate _{solution} impregnation of LSF cathode	0–15 μg/cm ²	550–650	+	[3]
C–V	(La _{0.8} Sr _{0.2}) _x FeO _{3–δ} (25–40 μm) + Ce _{0.8} Sm _{0.2} O _{1.9} (5 μm) on 8YSZ (5–10 μm) (anode-supported) (active area: 3.8 cm ²)	Pd diamine nitrite added to LSF nitrate _{solution} ; metallic Pd _{powder} added to LSF powder	2 vol.%	700–850	+	[4]
C–V + ac impedance	La _{0.6} Sr _{0.4} Fe _{0.8} Co _{0.2} O ₃ + Ce _{0.8} Gd _{0.2} O _{1.9} (20–25 μm) on Ce _{0.8} Sm _{0.2} O _{1.9} (2 mm) (active area: 1.1 cm ²)	AgNO ₃ _{solution} impregnation of LSF–CGO cathode	10–15 mg/cm ²	500–700	+	[5,6]
ac impedance	Pt–Sc _{0.10} Ce _{0.01} Zr _{0.89} O ₂ (15–120 μm) on 8YSZ (2 mm) (active area: 0.3 cm ²)	Pt powder mixed with SSZ powder	SSZ/Pt ratio: 0.05–0.6 wt.%	550–900	+	[7]
C–V	(La _{0.8} Sr _{0.2}) _x FeO _{3–δ} (25–40 μm) + Ce _{0.8} Sm _{0.2} O _{1.9} (5 μm) on 8YSZ (5–10 μm) (anode-supported) (active area: 3.8 cm ²)	Pt diamine nitrite added to LSF nitrate _{solution} ; metallic Pt _{powder} added to LSF powder	1–2 vol.%	700–800	0	[8]
C–V	La _{0.85} Sr _{0.15} MnO ₃ (20 μm) on (3–8)YSZ (1 mm) (active area: 0.3 cm ²)	LSM impregnated with [Pt(NH ₃) ₄]Cl ₂	100 μg/cm ²	800–1000	+	[9,10]
C–V	La _{0.6} Sr _{0.4} CoO ₃ (16–20 μm) + Ce _{0.8} Sm _{0.2} O _{1.9} (1 μm) on 8YSZ (1 mm) (active area: 0.3 cm ²)	LSC impregnated with [Pt(NH ₃) ₄]Cl ₂	100 μg/cm ²	800–1000		[11]
ac impedance	La _{0.8} Sr _{0.2} Co _{0.6} Fe _{0.4} O ₃ (50–120 μm) on Ce _{0.8} Gd _{0.2} O _{1.9} (2 mm) (active area: 0.28 cm ²)	Pt powder mixed with LSCF powder	LSCF/Pt ratio: 20/80–95/5 wt.%	600–900	+	[12]
ac impedance	Pt–Sc _{0.10} Ce _{0.01} Zr _{0.89} O ₂ (180 μm) on 8YSZ (2 mm) (active area: 0.3 cm ²)	Pt–Ag powder mixed with SSZ powder	SSZ/Pt–Ag ratio: 0.1–0.9 wt.%	550–900	+	[13]

C–V, current–voltage.

(semi-logarithmic plots of the current–potential curves) obtained at 800 °C on an 8YSZ electrolyte (thickness: 130 μm) with a La_{0.84}Sr_{0.16}MnO₃ cathode layer (thickness: 50 μm, diameter: 10 mm) on both sides. Highly dispersed Pd (≤0.1 mg/cm²) was added on both sides by means of an aqueous solution of Pd. Other studies [3,4] focussed on the addition of palladium to lanthanum-ferrite-type SOFC cathodes. This type of cathode material is a perovskite with both high ionic and electronic conductivity. This means that the exchange reaction of oxygen from the gas phase to the oxide ion can take place on a larger part of the surface area of this cathode material and is not restricted to the three-phase boundary as it is for a La_{0.65}Sr_{0.30}MnO₃ (LSM)–YSZ-based SOFC. Consequently, for this type of lanthanum-ferrite-based SOFC cathode the addition of noble metals to the cathode layer can probably further improve the oxygen exchange processes. Here, Sahibzada et al. [3] based their conclusions on ac impedance spectroscopic measurements performed in the

range 400–750 °C with a self-supporting Ce_{0.9}Gd_{0.1}O_{1.95} electrolyte and a porous La_{0.6}Sr_{0.4}Co_{0.2}Fe_{0.8}O₃ cathode on both sides. Furthermore, current–voltage measurements between 550 and 650 °C were made using a precision potentiostat on Ni-cermet-anode-supported single cells with a Ce_{0.9}Gd_{0.1}O_{1.95} electrolyte (thickness: 5 μm) and a La_{0.6}Sr_{0.4}Co_{0.2}Fe_{0.8}O₃ cathode. For both types of cells Pd was added (0–15 μg/cm²) by impregnation using Pd nitrate dissolved in nitric acid. Positive effects in relation to the presence of Pd (50% power density improvement at 700 mV and 700 °C) were also reported by Simner et al. [4]. In their study, small single cells (active diameter: 19.5 mm) were used. These cells were based on a Ni-cermet anode, followed by a NiO–8YSZ anode functional layer (thickness: 5–10 μm), an 8YSZ electrolyte (thickness: 5–10 μm), a Ce_{0.8}Sm_{0.2}O_{1.9} interlayer (thickness: 5 μm), and a La_{0.8}Sr_{0.2}FeO_{3–δ} cathode (25–40 μm). Current–voltage data were obtained by using a potentiostat–galvanostat electrochemical testing unit.

With respect to the catalytic benefits of the addition of small amounts of silver to the cathode of SOFCs, only a small number of studies can be found [5–7]. A first approach was made by Wang et al. [5] by adding Ag (infiltration using AgNO_3) to a $\text{La}_{0.6}\text{Sr}_{0.4}\text{Co}_{0.8}\text{Fe}_{0.2}\text{O}_3\text{--Ce}_{0.8}\text{Gd}_{0.2}\text{O}_{1.9}$ composite cathode (20 μm , 30 wt.% CGO, 10–15 mg/cm^2 Ag). The electrolyte consisted of $\text{Ce}_{0.8}\text{Sm}_{0.2}\text{O}_{1.9}$. A Ni-ceria electrode was used as the anode. From the three-probe ac impedance measurements, performed between 500 and 700 °C, it was concluded that small amounts of Ag can significantly enhance the cathode activity. This was explained by an improvement of the surface exchange step of oxygen from the gas phase into the oxide. Probably, Ag particles improve the electron supply and oxygen adsorption. Additional information about these three-probe complex impedance measurements on the LSFC–CGO–Ag system can be found in Ref. [6].

Other model studies including, e.g., impedance spectroscopy or current interruption methods and concerning the influence of Pt on the polarization characteristics of different types of cathodes can be found elsewhere [2,7–13]. For example, positive effects were reported by Sasaki et al. [7] dealing with polarization characteristics using ac impedance spectroscopy of Pt– $\text{Sc}_{0.10}\text{Ce}_{0.01}\text{Zr}_{0.89}\text{O}_2$ -cermet cathodes (thickness: up to 120 μm , Pt ratio: up to 0.60 wt.%, diameter: 6 mm) applied on both sides of a YSZ electrolyte (thickness: 2 mm). The temperature range was between 550 and 900 °C. Here, impedance measurements revealed a lower activation energy (E_a) of the cathode reaction in the presence of Pt. These studies showed that in general the addition of small amounts of Pt to the cathode enhances the cathode performance by improving the oxygen surface reaction rates. In all cases, the overpotential of cathodes loaded with Pt was lower than that of corresponding Pt-free cathodes.

Based on the results described above, a study was initiated to increase the power output of the state-of-the-art cells manufactured at Forschungszentrum Jülich by the addition of either Pd, Ag, or Pt. The specific concentration ranges of the noble metals added to the cathode used in this study are generally based on data already published in the literature [2–13].

2. Experimental

2.1. Preparation of cells

2.1.1. Basic aspects

The basis of both noble-metal-containing and reference cells with dimensions of 50 mm \times 50 mm consisted of an anode substrate (thickness: \sim 1500 μm), an anode functional layer (thickness: 5–10 μm), and an electrolyte (thickness: 5–10 μm). The anode substrate, a porous cermet consisting of Ni and 8 mol% yttria-stabilized zirconia (8YSZ), was produced by warm pressing using a so-called Coat-Mix[®]

material and pre-sintered at 1200 °C [1,14,15]. NiO as the precursor of Ni was purchased from Baker, USA, and 8YSZ was obtained from Unitec, UK. Afterwards, the anode functional layer (Ni/8YSZ) and the electrolyte (8YSZ) were both deposited by vacuum slip casting and co-fired at 1400 °C. On top of the electrolyte the cathode functional layer (CFL) with LSM and 8YSZ as base materials and the cathode layer (LSM) were applied by screen printing. 8YSZ used for the electrolyte and the cathode functional layer was obtained from Tosoh, Japan. The surface area of both layers, also termed as the active surface area, was 40 mm \times 40 mm. More details of the manufacturing processes for the Jülich anode-supported design can be found in Ref. [16].

Pastes for the screen printing process to apply the CFL and the cathode layer were prepared by mixing the corresponding powders with a binder consisting of ethyl cellulose in terpineol.

The LSM powder used for both the CFL and the cathode was synthesized by a spray drying process [1,17] using nitrate salts, i.e. $\text{La}(\text{NO}_3)_3 \cdot 6\text{H}_2\text{O}$, $\text{Sr}(\text{NO}_3)_2$, and $\text{Mn}(\text{NO}_3)_2 \cdot 4\text{H}_2\text{O}$ except in the case of series Ag-B (see Section 2.1.3), followed by a calcination step for 3 h to obtain the perovskite phase. A calcination temperature of 900 °C was chosen for the powder used for the preparation of the CFLs and cathode layers that were co-fired at 1100 °C, while a calcination temperature of 700 °C was chosen for the powder used for the preparation of the CFLs and cathode layers that were co-fired at 920 °C (see Sections 2.1.2–2.1.5).

In the following sections the preparation of the differently modified cathodes is described.

2.1.2. Pd-containing cells

Two routes were used to add Pd to the CFL. On the one hand, LSM and YSZ (60/40 wt.%) were mixed with either Pd black or Pd on activated carbon (Pd-C) to obtain a Pd amount of 2 and 0.1 wt.%, respectively. After deposition of the CFL and the cathode layer, the layers were co-fired at 1100 °C for 3 h resulting in a thickness of 7 and 35 μm , respectively. On the other hand, a conventional cell (see Section 2.1.5) was infiltrated with a Pd nitrate solution (1 g $\text{Pd}(\text{NO}_3)_2/1 \text{H}_2\text{O}$), corresponding to 5 $\mu\text{g Pd}/\text{cm}^2$ electrode area. After infiltration, the cell was calcined at 600 °C for 3 h to decompose the nitrate.

2.1.3. Ag-containing cells

Addition of Ag to the cathode was performed by two different methods. The two series of single cells produced according to these two methods will be named “series Ag-A” and “series Ag-B” hereafter.

In the case of series Ag-A, Ag was added to the CFL by mixing LSM and 8YSZ with different Ag compounds including pure Ag powder (0.5–1 μm , Alfa Aesar, Germany, 99.9%), Ag_2O (Alfa Aesar, >99%), Ag acetate (MaTeck, Germany, >99%), Ag citrate ($\text{Ag}_3\text{C}_6\text{H}_5\text{O}_7 \cdot \text{H}_2\text{O}$, Alfa Aesar, puriss.), Ag_2CO_3 (MaTeck, 99.7%), colloidal Ag (Merck,

Germany, puriss.), and AgNO_3 (Merck, 99.8%). The ratio Ag/8YSZ/LSM was set at 33/33/33 vol.%.

In the case of series Ag-B, Ag was added to the CFL by using LSM that was synthesized with the addition of small amounts of AgNO_3 . This type of LSM perovskite will be named “LSM:Ag” hereafter. Four LSM:Ag powders with Ag amounts of 0.1, 0.5, 1.0, and 2.0 wt.% were synthesized. These powders were used for the preparation of the CFL (60/40 wt.% LSM:Ag/8YSZ). Synthesis of the powders was performed according to the citrate complexation or Pechini method [18]. First, nitrate salts of La, Sr, Mn, and Ag (Merck, puriss.) were dissolved in deionized water, followed by complexation of the cations using citric acid in excess (>2 mol/mol cation). Afterwards, polyesterification was performed by adding ethylene glycol in excess (>5 mol/mol citric acid). Next, the solution was smoothly heated to remove all excess liquid and to decompose the nitrate and organic compounds. Finally, the powders thus obtained were calcined at 700°C for 3 h to obtain the perovskite phase.

The cathode functional layer (thickness: 15–20 μm) and the cathode layer (thickness: 45–50 μm) of both series of Ag-containing cells were co-fired at 920°C for 3 h. This relatively low sintering temperature had to be chosen because of the low melting point of Ag (962°C).

2.1.4. Pt-containing cells

Pt was added either directly on top of the electrolyte layer or by a mixing procedure. With respect to the first method a solution of Pt in nitro-hydrochloric acid (concentration of dissolved metal in the solution: 5 g/l) was dropped onto the electrolyte resulting in a platinum quantity of 150 $\mu\text{g}/\text{cm}^2$. Next, the samples were heated to 700°C in air to obtain metallic platinum. Subsequently, the CFL (thickness: 7 μm , 60/40 wt.% LSM/8YSZ) and the LSM cathode layer (thickness: 35 μm) were screen-printed onto the platinum deposit and co-fired at 1100°C for 3 h.

In the case of the second method, LSM and YSZ for the CFL were mixed with Pt black, resulting in a quantity of 2 wt.%. Co-firing of the modified cathode functional layer (Pt/LSM/YSZ) and the cathode layer (LSM) was performed at 1100°C for 3 h. The thicknesses of these layers were 7 and 35 μm , respectively.

2.1.5. Noble-metal-free cells

Three types of cells without the addition of noble metals were prepared as reference cells. In all cases the composition of the CFL was 60/40 wt.% LSM/8YSZ with a cathode layer consisting of pure LSM.

The first type of reference cell will be named ‘conventional cells’ in the following because this type corresponds to the state-of-the-art cells manufactured at Forschungszentrum Jülich. Co-firing of the CFL and the cathode layer was performed at 1100°C for 3 h. The thicknesses of the two layers after sintering were 15–20 and 45–50 μm , respectively.

To separate the influence of the addition of Pd and Pt addition from the thickness of the CFL and cathode layer,

a second type of reference cell was prepared with a 7 μm thick cathode functional layer and a 35 μm thick cathode layer. The two layers were co-fired at 1100°C for 3 h. This type of reference cell is named ‘Pt-free cells’ or ‘Pd-free cells’ in the following.

To separate the influence of the addition of Ag from the sintering temperature, the CFL and the cathode layer of a third type of reference cell were co-fired at 920°C for 3 h. The thicknesses of the layers were 15–20 and 45–50 μm , respectively. This type of cell is named ‘Ag-free cells’ in the following.

2.2. Electrochemical measurements

Electrochemical measurements of the single cells were performed in an alumina test housing placed inside the furnace. In order to obtain sufficient electronic contact between the cell and the electronic devices, at the anode side a Ni mesh and at the cathode side a Pt mesh were used. Sealing of the gas compartment was obtained by a gold seal. At the beginning of the tests an argon flow was introduced at the anode side and an air flow at the cathode side. The temperature was then slowly increased to the temperature for anode reduction. After reaching this temperature, the anode of the single cells was reduced by replacing the argon with hydrogen stepwise. Water vapor (3 vol.%) was added by saturating the hydrogen gas through a water bubbler and condenser (super saturation and condensation) at the desired dew point (24°C). The total gas flows of hydrogen and air were both set at 1000 ml/min (standard temperature and pressure (STP)) using mass flow controllers. The electrochemical performance was measured between 650 and 800°C . All electrochemical data are obtained by dc methods using a current-controlled power supply type Gossen 62N—SSP500-40 (Gossen-Metrawatt GmbH, Germany) and a computer-controlled data acquisition system including a datalogger type NetDAQ 2640A (Fluke, The Netherlands). The current–voltage characteristics were measured with increasing current load by a sequential step change of $0.0625\text{ A}/\text{cm}^2$ starting from zero until the voltage dropped below 0.7 V or until the maximum current load of $1.25\text{ A}/\text{cm}^2$ was reached. A comparison of the electrochemical performance between the different type of single cells was made by comparing the current densities at 0.7 V. These calculations of the current density at 700 mV (for $I > 1.25\text{ A}/\text{cm}^2$) and at exact temperatures, i.e. 650, 700, 750, 800, 850 and 900°C , are based on inter- or extrapolation using a second- or third-order polynomial function. Calculations of the area-specific resistance are based on linear regression of the current–voltage curves at 0.7 V.

2.3. Characterization

The stoichiometry of the LSM powders was controlled by ICP-OES and the phase purity by X-ray diffraction (Siemens D 500). Scanning electron microscopic (SEM) analysis of

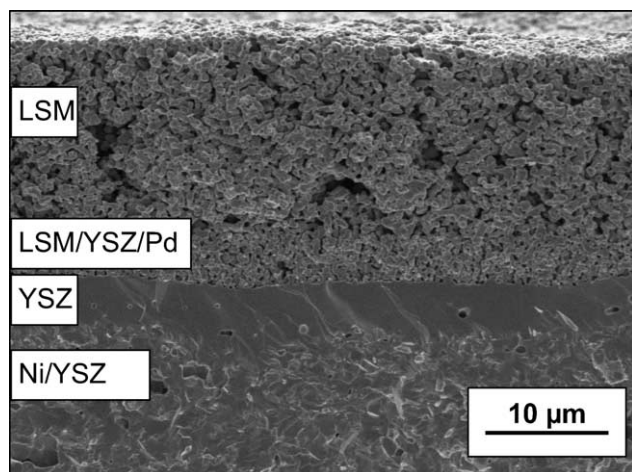


Fig. 1. SEM micrograph of the fracture surface of a cell with 2 wt.% Pd in the cathode functional layer.

polished cross-sections and fracture surfaces was performed using a LEO 1530 electron microscope (Gemini).

3. Results

3.1. Pd-containing cells

3.1.1. Microstructure

The fracture surface of a single cell containing 2 wt.% Pd black in the CFL is shown in Fig. 1. The different layers can clearly be seen with a porous cathode layer (LSM) on the top, followed by a denser CFL including 2 wt.% Pd black, the electrolyte (YSZ), and the anode substrate (Ni/YSZ-cermet) including an anode functional layer. No obvious differences between the microstructure of this cell and that of the other single cells, i.e. Pd-free and with 0.1 wt.% Pd-C, were found.

3.1.2. Current–voltage measurements

Fig. 2 shows current–voltage curves at different temperatures for a conventional SOFC. Fig. 3 depicts the current density at 700 mV of Pd-containing cells in comparison to the

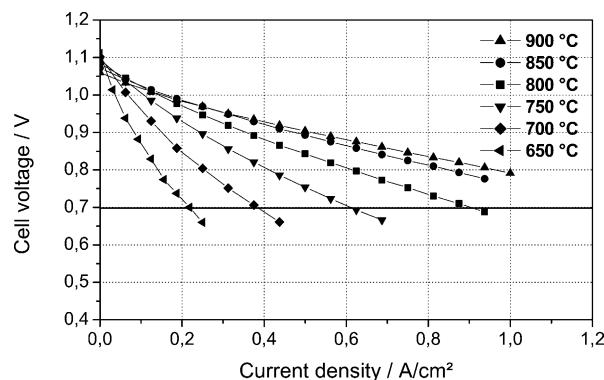


Fig. 2. Current–voltage curves for a conventional 16 cm² anode-supported single cell as a function of the temperature.

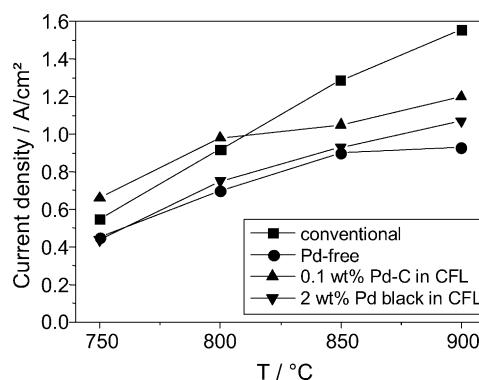


Fig. 3. Current density at 700 mV of Pd-containing cells in comparison to a conventional and a Pd-free cell as a function of the temperature.

conventional cell and a Pd-free cell as a function of the temperature. The current densities at 700 mV and the calculated area-specific resistance of the different types of single cells are listed in Table 2. No catalytic effect was observed with single cells containing Pd black, whereas Pd-C-containing cells showed a significant improvement in electrochemical performance, in particular at lower temperatures. The current densities of this type of single cell were significantly higher than that found for Pd-free SOFCs.

Table 2

Electrochemical data of Pd-containing single cells in comparison to conventional cells and Pd-free cells

T (°C)	Conventional	Pd-free	Pd-C (0.1 wt.%)	Pd black (2 wt.%)	Pd(NO ₃) ₂
Current density at 700 mV (A/cm ²)					
900	1.56 ± 0.18	0.94 ± 0.03	1.22 ± 0.04	1.06 ± 0.06	n.m.
850	1.29 ± 0.11	0.89 ± 0.03	0.92 ± 0.03	0.91 ± 0.04	n.m.
800	0.92 ± 0.05	0.70 ± 0.04	0.97 ± 0.19	0.73 ± 0.05	0.74 ± 0.01
750	0.55 ± 0.11	0.45 ± 0.03	0.67 ± 0.05	0.40 ± 0.03	0.53 ± 0.01
Area-specific resistance (mΩ cm ²)					
900	206 ± 27	330 ± 7	247 ± 6	266 ± 9	n.m.
850	252 ± 27	361 ± 8	331 ± 7	331 ± 9	n.m.
800	343 ± 64	418 ± 12	168 ± 23	374 ± 15	484 ± 10
750	517 ± 174	635 ± 18	248 ± 11	640 ± 25	648 ± 5

Fuel: H₂ with 3 vol.% H₂O, oxidant: air; n.m.: not measured.

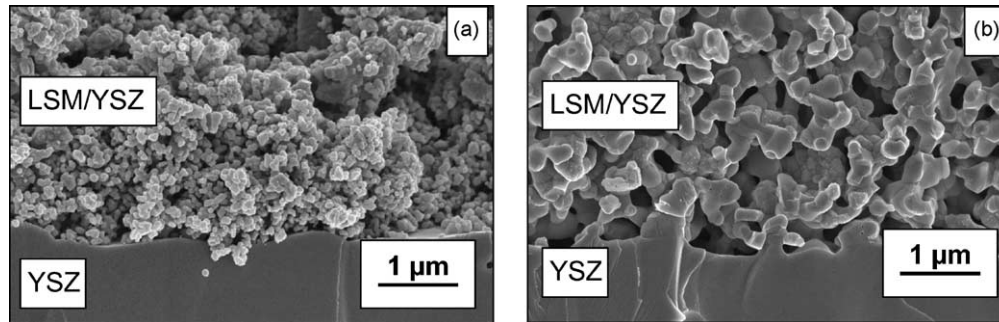


Fig. 4. SEM micrograph of the fracture surface of (a) an Ag-free cell sintered at 920 °C and (b) a conventional cell (sintering temperature = 1100 °C).

In addition, conventional cells were impregnated with $\text{Pd}(\text{NO}_3)_2$ solution. Here, no improvement in the current density was obtained.

3.2. Ag-containing cells

3.2.1. Microstructure

Fig. 4a and b shows micrographs of the fracture surface of two cells, one sintered at 920 °C and the other at 1100 °C. The microstructure of the Ag-free cell sintered at 920 °C differs from that observed for the conventional cell. This very fine-grained microstructure after sintering at 920 °C was found independently of the synthesis route (series Ag-A or Ag-B). After sintering at 1100 °C well-developed sintering necks were formed between electrolyte and cathode functional layer, whereas after sintering at 920 °C such sintering necks cannot be observed.

Fig. 5a–c shows polished cross-sections of cells prepared with Ag powder, Ag_2O , and Ag citrate, respectively, in the CFL. These micrographs were obtained with backscattered electrons. In the order Ag powder– Ag_2O –Ag citrate an increasing amount of pores can be observed in the CFL. A high amount of large pores was also observed in the CFL of the cells prepared with colloidal Ag, Ag acetate, Ag_2CO_3 , and AgNO_3 .

3.2.2. Current–voltage measurements

In Fig. 6 the current densities at 800 and 700 mV of the cells of series Ag-A are shown in comparison to a conventional and an Ag-free cell. The highest current density ($0.92 \pm 0.05 \text{ A/cm}^2$) was obtained with the conventional cell. The electrochemical performance of the Ag-containing cells decreased in the following order of Ag additives: Ag powder > Ag_2O > Ag acetate > Ag_2CO_3 > AgNO_3 . The cells prepared with the addition of Ag citrate and Ag colloidal totally failed. Comparing the current densities of the Ag-containing cells with those of the Ag-free cell, only the addition of Ag powder and Ag_2O resulted in an improved electrochemical performance. A detailed overview of the electrochemical data between 750 and 900 °C as a function of the temperature is given in Table 3.

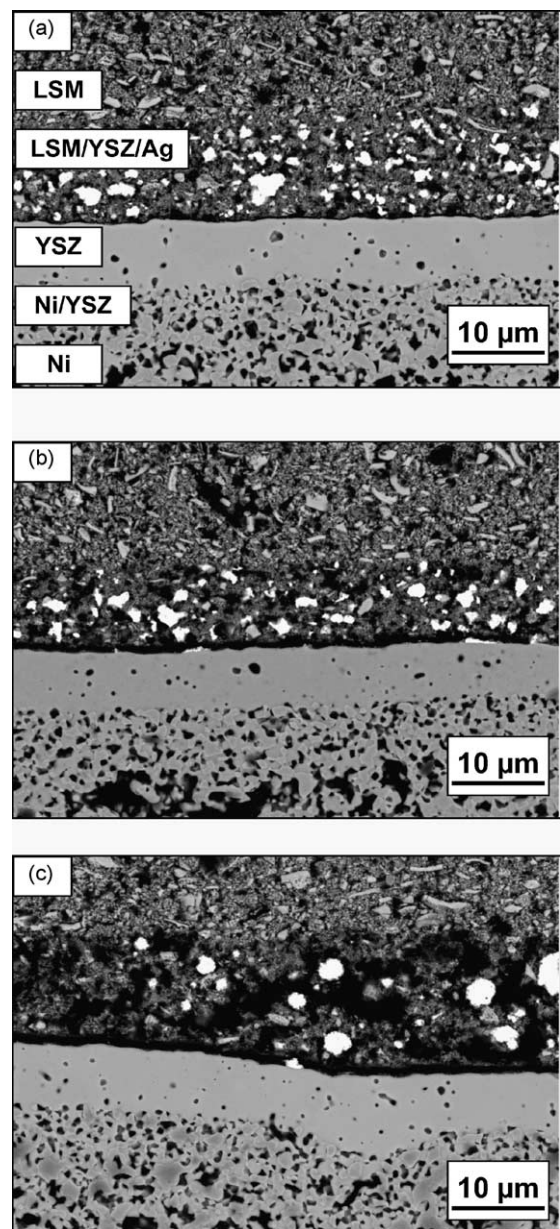


Fig. 5. SEM micrographs in backscattering mode of cells prepared with (a) Ag powder, (b) Ag_2O , and (c) Ag citrate in the CFL.

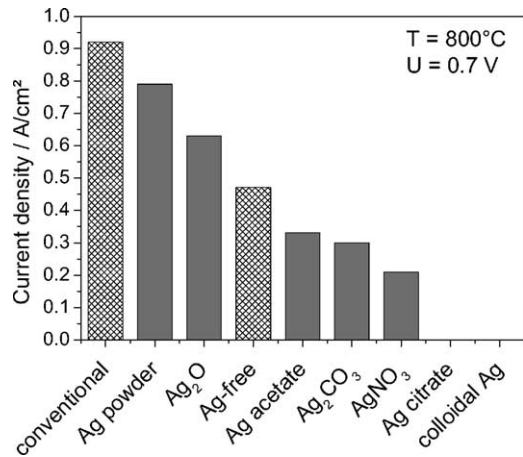


Fig. 6. Current densities of cells prepared with different Ag precursors (series Ag-A) in comparison to a conventional and an Ag-free cell.

Table 4 lists the electrochemical data between 700 and 800 °C of the cells of series Ag-B in comparison to those of the Ag-free cell. The current densities obtained with cells of series Ag-B were at the same level as those measured for the Ag-free cells. At 800 °C the current density was nearly independent of the Ag concentration. Apparently, a slight improvement was obtained at lower temperatures.

Table 3
Electrochemical data of the cells of series Ag-A in comparison to conventional and Ag-free cells

T (°C)	Conventional	Ag-free	Ag powder	Ag ₂ O	Ag acetate	Ag ₂ CO ₃	AgNO ₃
Current density at 700 mV (A/cm ²)							
900	1.56 ± 0.18	0.84 ± 0.09	1.67 ± 0.09	–	0.63 ± 0.12	0.51 ± 0.05	0.41 ± 0.04
850	1.29 ± 0.11	0.66 ± 0.05	1.22 ± 0.08	0.80 ± 0.12	0.53 ± 0.03	0.46 ± 0.04	0.28 ± 0.02
800	0.92 ± 0.05	0.49 ± 0.03	0.83 ± 0.10	0.63 ± 0.13	0.25 ± 0.02	0.27 ± 0.03	0.22 ± 0.01
750	0.55 ± 0.11	0.28 ± 0.02	–	–	0.16 ± 0.00	0.15 ± 0.01	0.16 ± 0.01
Area-specific resistance (mΩ cm ²)							
900	206 ± 27	396 ± 36	136 ± 5	–	256 ± 27	510 ± 24	624 ± 32
850	252 ± 27	524 ± 34	194 ± 8	173 ± 1	363 ± 7	797 ± 34	1018 ± 32
800	343 ± 64	752 ± 22	234 ± 15	290 ± 32	1048 ± 51	1200 ± 46	1648 ± 28
750	517 ± 174	1331 ± 66	–	–	2016 ± 92	2344 ± 79	2525 ± 26

Fuel: H₂ with 3 vol.% H₂O, oxidant: air.

Table 4
Electrochemical data of the cells of series Ag-B in comparison to Ag-free cells

T (°C)	Ag-free	Ag: 0.1 wt.%	Ag: 0.5 wt.%	Ag: 1.0 wt.%	Ag: 2.0 wt.%
Current density at 700 mV (A/cm ²)					
800	0.49 ± 0.03	0.52 ± 0.01	0.54 ± 0.01	0.39 ± 0.01	0.49 ± 0.01
750	0.28 ± 0.02	0.41 ± 0.01	0.43 ± 0.01	0.31 ± 0.02	0.38 ± 0.01
700	n.m.	0.24 ± 0.01	0.23 ± 0.02	0.19 ± 0.01	0.23 ± 0.01
Area-specific resistance (mΩ cm ²)					
800	752 ± 22	651 ± 4	581 ± 8	834 ± 13	683 ± 8
750	1331 ± 66	832 ± 5	768 ± 10	1112 ± 32	872 ± 6
700	n.m.	1432 ± 42	1384 ± 60	1648 ± 55	1432 ± 14

Fuel: H₂ with 3 vol.% H₂O, oxidant: air; n.m.: not measured.

3.3. Pt-containing cells

3.3.1. Microstructure

Fig. 7a shows an SEM micrograph depicting platinum on top of the electrolyte. Here, as pointed out in Section 2.1.4, Pt was applied by dropping Pt-containing nitro-hydrochloric acid on the electrolyte surface. Particles with a size of less than 0.1 μm up to agglomerates with a size of several microns can be observed. After subsequently screen printing and co-firing of the CFL and the cathode layer, platinum particles are still visible near the cathode/electrolyte interface, as can be seen in Fig. 7b.

The microstructure of the cathode containing 2 wt.% Pt was similar to that of the Pd-containing cell (see Fig. 1).

3.3.2. Current–voltage measurements

The current densities measured at 700 mV and the area-specific resistances of the different types of single cells are listed in Table 5. Additionally, Fig. 8 shows the current densities of Pt-containing cells in comparison to those of a conventional cell and a Pt-free cell as a function of the temperature. The highest performance was obtained with the conventional single cell, whereas the lowest was found for the single cell with Pt black added to the CFL. The current densities of the single cell with Pt added by deposition on the electrolyte was the same as those of the Pt-free cell.

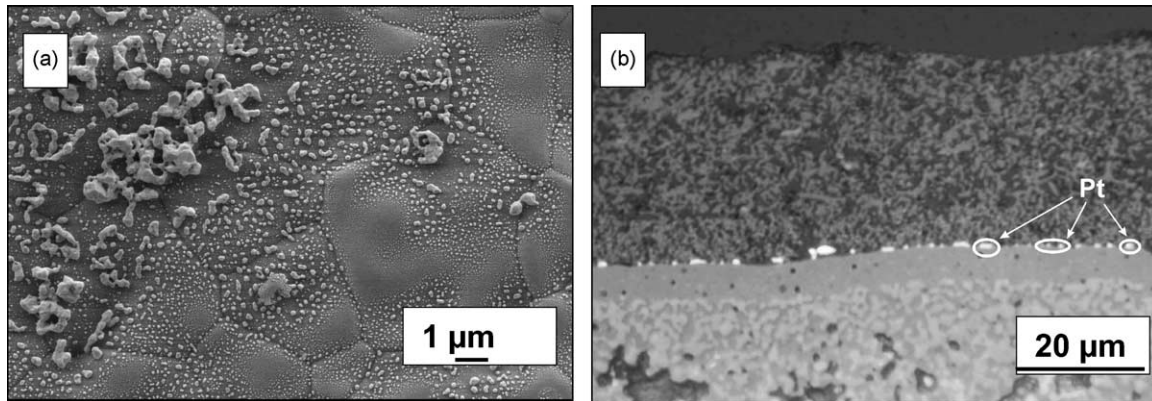


Fig. 7. SEM micrographs of (a) the outer surface of the electrolyte layer after applying Pt with the use of a nitro-hydrochloric acid solution and (b) cross-section of a single cell after sintering with Pt particles (white spots) at the cathode/electrolyte interface.

Table 5
Electrochemical data of Pt-containing single cells in comparison to conventional cells and Pt-free cells

T ($^{\circ}\text{C}$)	Conventional	Pt-free	Pt in HNO_3/HCl	Pt black
Current density at 700 mV (A/cm^2)				
900	1.56 ± 0.18	0.94 ± 0.03	0.86 ± 0.02	0.79 ± 0.03
850	1.29 ± 0.11	0.89 ± 0.03	0.88 ± 0.07	0.74 ± 0.02
800	0.92 ± 0.05	0.70 ± 0.04	0.68 ± 0.02	0.55 ± 0.12
750	0.55 ± 0.11	0.45 ± 0.03	0.47 ± 0.01	0.39 ± 0.05
Area-specific resistance ($\text{m}\Omega \text{cm}^2$)				
900	206 ± 27	330 ± 7	344 ± 5	388 ± 9
850	252 ± 27	361 ± 8	343 ± 17	418 ± 6
800	343 ± 64	418 ± 12	453 ± 1	552 ± 11
750	517 ± 174	635 ± 18	600 ± 6	845 ± 11

Fuel: H_2 with 3 vol.% H_2O , oxidant: air.

4. Discussion

The results show that in comparison to the Pd-free single cell, the power density of single cells with 0.1 wt.% Pd-C added to the CFL was increased. In particular at lower temperatures, i.e. 750 and 800 $^{\circ}\text{C}$, the relative improvement was even more pronounced. This points to an increasing catalytic

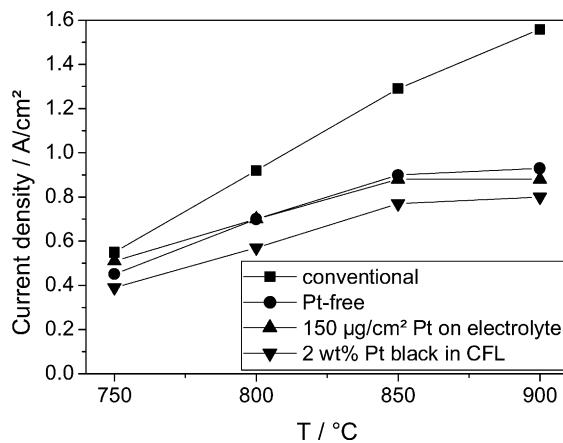


Fig. 8. Current density at 700 mV of Pt-containing cells in comparison to a conventional and a Pt-free cell as a function of the temperature.

effect of Pd in comparison to LSM with decreasing temperature. Similar results were also reported by Sahibzada et al. [3]. As a result, the influence of palladium becomes more effective at lower operating temperatures.

No obvious improvement of the electrochemical performance was obtained with Pd black. Reasons for the different behavior of these Pd-containing cells are not yet clear, but it is likely that a lower specific surface area of Pd black in comparison to Pd-C led to a lower surface area coated with Pd, and consequently to no improvement. In addition, the Pd-free single cell showed a lower performance in comparison to the conventional single cell. This can be explained by differences in the thickness of the CFL. Conventional SOFCs contain a CFL with a thickness of 15–20 μm , whereas that of the Pd-free single cell was about 7 μm . Wilkenhöner et al. [19] reported a strong increase of the overpotentials for CFLs (LSM + 40 wt.% 8YSZ) with a thickness of less than about 10 μm . In the case of a layer thickness between 10 and 35 μm , no obvious changes were found in the electrochemical activity. Therefore, it is likely that the length of three-phase boundaries for the Pd-free single cell is lower than that of the conventional single cell, thus causing a lower electrochemical performance.

However, an attempt to prepare cells with a thicker CFL including small amounts of Pd-C was not successful. In

this case, the cathode was partially spalled after sintering, probably due to oxidation of the carbon.

In addition, another method was used to add small amounts of palladium to the cathode layer of conventional-type SOFC by infiltration with $\text{Pd}(\text{NO}_3)_2$. However, this did not influence the electrochemical behavior. Here, it is assumed that, in spite of large capillary forces, this is due to an insufficient infiltration of the palladium solution into the fine-structured CFL.

Compared with the Ag-free cell, cells treated with Ag powder and Ag_2O revealed a better performance. This indicates that the presence of 33 vol.% Ag might have some beneficial catalytic effect by positively influencing the surface exchange reaction of oxygen from the gas phase to the oxide. However, the electrochemical performance of these cells was still significantly lower than that of the conventional cell. This lower performance can be explained by a weaker contact between the electrolyte and the CFL and a poor intergranular connection in the CFL (see Fig. 4), both due to the lower sintering temperature, i.e. 920°C instead of 1100°C . Cells prepared with the other Ag precursors, i.e. Ag acetate, Ag_2CO_3 , AgNO_3 , Ag citrate, and colloidal Ag, all showed a lower electrochemical performance than the Ag-free single cell. Here, not only the lower sintering temperature but also the formation of a high amount of large pores plays an important role leading to the low performance. This is supported by the fact that the amount of pores correlated well with the current density, i.e. the higher the porosity the lower the current density. A higher porosity of the CFL will finally result in a lower specific contact area between the electrolyte and the CFL as well as a lower amount of active three-phase boundaries detrimentally influencing the electrochemical performance.

The addition of Ag by synthesis following the Pechini method (series Ag-B) did not result in an obvious improvement of the electrochemical performance either, although metallic Ag could be detected in small amounts by XRD after sintering [20]. Only at 750°C a slight improvement found. Since the microstructure of the CFL corresponded well to that of the Ag-free single cells, it can be concluded that the concentration of Ag in the CFL was probably not sufficient or that Ag was not dispersed finely enough to induce the desired catalytic effect.

Regarding the Pt-containing SOFCs, the electrochemical measurements clearly show that no improvement in the performance was obtained by the presence of small amounts of Pt, either added by deposition on the electrolyte or by mixing with the YSZ/LSM powder (see Table 5). Probably the amount or the dispersion of Pt on the electrolyte surface and in the CFL was too low to influence the electrochemical performance. The higher performance of the conventional cell compared to the other cells is probably due to a thicker CFL as in the case of the Pd-containing single cells.

From the data above it is clear that under the given experimental conditions several conclusions can be drawn regarding the influence of different noble metals on the

electrochemical performance of anode-supported single cells. This can partly be explained by differences in the electrochemical and catalytic properties of the added elements, by different routes of addition including the local presence of noble metals, and differences in the concentration. In addition, results from the experiments described in this paper do not always correspond to those already published. Since different groups performed experiments with different model systems, different geometric dimensions, and different compositions of the cathode and/or cathode functional layer (a short overview is given in Table 1), on the one hand, it is very difficult to draw final conclusions about the influence of each noble metal, but, on the other hand, data already published can be used as important input parameters for further development to improve the electrochemical performance of complete SOFCs.

5. Conclusions

- With respect to Pd-containing single cells, only cells with Pd-C showed an improvement in the electrochemical performance, which was more pronounced at lower temperatures. This increasing catalytic effect of Pd with decreasing temperature can be explained by the fact that the cathode surface reactions are enhanced.
- In comparison to Ag-free single cells, an improvement in the electrochemical performance was obtained by adding 33 vol.% Ag using pure Ag powder or Ag_2O , indicating that Ag is an electrocatalytically active element. However, in comparison to conventional cells, the power output was lower. This was due to a lower sintering temperature of the Ag-containing single cells because of the low melting point of Ag. Consequently, a weak adhesion and thus insufficient contact including a low lateral electronic contact of the CFL caused the lower performance.
- The use of Ag compounds, i.e. Ag acetate, Ag_2CO_3 , AgNO_3 , Ag citrate, and colloidal Ag, resulted in a lower performance than that obtained with Ag-free single cells. Here, decomposition of the precursor during sintering resulted in damage to the cathode functional layer by severe pore formation.
- The addition of small amounts of Ag (0.1–2.0 wt.%) to the cathode functional layer by synthesis following the Pechini method did not result in a significant improvement of the electrochemical performance.
- Addition of Pt did not positively affect the electrochemical performance.

Acknowledgements

The present study was financially supported by the German Federal Ministry of Education and Research (BMBF) under contract no. 01SF0039. In addition, the authors would like to thank Mr. W. Jungen for the synthesis of the

spray-dried LSM, Mr. M. Kampel and Mr. G. Blaß for the preparation of anode substrates and the electrolyte, and Mr. M. Kappertz for metallographic sample preparation.

References

- [1] H.P. Buchkremer, U. Dieckmann, D. Stöver, in: B. Thorstensen (Ed.), Proceedings of the Second European Solid Oxide Fuel Cell Forum, Oslo, Norway, 6–10 May 1996, European Fuel Cell Forum, Oberrohrdorf, Switzerland, p. 221.
- [2] J.W. Erning, T. Hauber, U. Stimming, K. Wippermann, J. Power Sources 61 (1996) 205–211.
- [3] M. Sahibzada, S.J. Benson, R.A. Rudkin, J.A. Kilner, Solid State Ionics 113–115 (1998) 285–290.
- [4] S.P. Simner, J.F. Bonnett, N.L. Canfield, K.D. Meinhardt, J.P. Shelton, V.L. Sprenkle, J.W. Stevenson, J. Power Sources 113 (2003) 1–10.
- [5] S. Wang, T. Kato, S. Nagata, T. Honda, T. Kaneko, N. Iwashita, M. Dokiya, Solid State Ionics 146 (2002) 203–210.
- [6] S. Wang, T. Kato, S. Nagata, T. Kaneko, N. Iwashita, T. Honda, M. Dokiya, Solid State Ionics 152–153 (2002) 477–484.
- [7] K. Sasaki, J. Tamura, M. Dokiya, Solid State Ionics 144 (2001) 233–240.
- [8] S.P. Simner, J.F. Bonnett, N.L. Canfield, K.D. Meinhardt, J.L. Shelton, V.I. Sprenkle, J.W. Stevenson, in: Proceedings of the 2002 Fuel Cell Seminar on Fuel Cells—Reliable, Clean Energy for the World, Palm Springs, CA, 18–21 November 2002, p. 344.
- [9] M. Watanabe, H. Uchida, M. Shibata, N. Mochizuki, K. Amikura, J. Electrochem. Soc. 141 (1994) 342–345.
- [10] H. Uchida, M. Yoshida, M. Watanabe, J. Electrochem. Soc. 146 (1999) 1–7.
- [11] H. Uchida, S. Arisaka, M. Watanabe, Solid State Ionics 135 (2000) 347–351.
- [12] K. Sasaki, J. Tamura, H. Hosoda, T.N. Lan, K. Yasumoto, M. Dokiya, Solid State Ionics 148 (2002) 551–555.
- [13] K. Sasaki, J. Tamura, M. Dokiya, Solid State Ionics 144 (2001) 223–232.
- [14] D. Simwonis, A. Naoumidis, F.J. Dias, J. Linke, A. Moropoulou, J. Mater. Res. 12 (1997) 1508–1518.
- [15] D. Stöver, H.P. Buchkremer, F. Tietz, N.H. Menzler, in: J. Huijsmans (Ed.), Proceedings of the Fifth European Solid Oxide Fuel Cell Forum, Lucerne, Switzerland, 1–5 July 2002, European Fuel Cell Forum, Oberrohrdorf, Switzerland, p. 1.
- [16] R. Förthmann, G. Blaß, H.P. Buchkremer, in: U. Stimming, S.C. Singhal, H. Tagawa, W. Lehnert (Eds.), Proceedings of the Fifth International Symposium on Solid Oxide Fuel Cells (SOFC-V), Aachen, Germany, 2–5 June 1997, The Electrochemical Society, Pennington, NJ, p. 1003.
- [17] P. Kontouros, R. Förthmann, A. Naoumidis, G. Stochniol, E. Syskakis, Ionics 1 (1995) 40.
- [18] M.P. Pechini, US Patent 3330 697 (1967).
- [19] R. Wilkenhöner, W. Malléner, H.P. Buchkremer, Th. Hauber, U. Stimming, in: B. Thorstensen (Ed.), Proceedings of the Second European Solid Oxide Fuel Cell Forum, Oslo, Norway, 6–10 May 1996, European Fuel Cell Forum, Oberrohrdorf, Switzerland, p. 279.
- [20] S. Uhlenbruck, F. Tietz, D. Sebold, H.P. Buchkremer, D. Stöver, Silver Incorporation into Cathodes for SOFC Operating at Intermediate Temperature, in press.